ELSEVIER

Chemical Engineering Journal 135 (2008) 232–237

Chemical Engineering Journal

www.elsevier.com/locate/cej

Fabrication and structural analysis of three-dimensionally well-ordered arrangements of silicon oxycarbide microparticles

Guoqing Guan [a], Katsuki Kusakabe [a,*], Haruka Ozono [a,b], Masatsugu Taneda [a], Masato Uehara [b], Hideaki Maeda [b]

[a] *Department of Living Environmental Science, Fukuoka Women's University, 1-1-1 Kasumigaoka, Higashi-ku, Fukuoka 813-8529, Japan*
[b] *Nanotechnology Research Institute, National Institute of Advanced Industrial Science and Technology (AIST), 807-1 Shuku-machi, Tosu, Saga 841-0052, Japan*

Received 7 February 2007; received in revised form 20 April 2007; accepted 21 April 2007

Abstract

A three-dimensionally (3D) well-ordered assembly composed of silicon oxycarbide (SiO_xC_y) microparticles was fabricated by an infiltration process using SiO_2 inverse opal structures as molds. Polycarbosilane was used as the precursor for the SiO_xC_y synthesis. The effect of the viscosity of polycarbosilane solution on the morphology of the fabricated SiO_xC_y microparticles and their assemblies was investigated. The ideal viscosity for the infiltration process was found to be approximately 2.0 mPa s. The structures of the SiO_xC_y microparticles obtained and their assemblies were analyzed by SEM, XRD, FT-IR, and N_2 adsorption. Each SiO_xC_y microparticle was bonded to neighboring microparticles by bridge formation, which could enhance the mechanical strength of the prepared SiO_xC_y microparticle assembly.

Keywords: Opals; Inverse opals; Microparticles; Microparticle assembly; Silicon oxycarbide; Macropores; Nanopores

1. Introduction

In recent years, the synthesis and arrangement of microspheres with a monodisperse size and shape distribution has received considerable attention [1–3]. Polymer microspheres fabricated with polystyrene (PS) and polymethylmethacrylate (PMMA) resins, and silica microspheres are typically used for these purposes because they are highly uniform. These types of microspheres and assemblies are usually used as photonic crystals [4,5], separation phases for chromatography [6], supports for immobilized enzymes [7], and an ordered array for DNA or protein separation [8]. Silicon carbide (SiC) is widely used in the ceramic and abrasive industry because of its high mechanical strength, thermal conductivity and stability, resistance toward oxidation, and the fact that it is chemically inert [9,10]. Silicon oxycarbide, a SiC-related material with the general formula SiO_xC_y, is also a good candidate for many applications due to its excellent chemical and thermomechanical stabilities [11–14]. It has been reported that the silicon oxycarbide is stable up to 1000–1200 °C and decomposes at higher temperatures to form nanocrystalline silicon carbide, graphite, and amorphous SiO_2 [14]. In the case of SiO_xC_y microparticles and assemblies thereof, interest is also driven by other potential applications such as catalyst supports in high temperature reactions [14,15] chromatographic packing materials for high performance liquid chromatography (HPLC). In HPLC applications, microparticles with sufficient rigidity to withstand the high packing pressure used are of prime importance [6]. To the best of our knowledge, although macroporous and mesoporous SiC-related ceramic structures have been fabricated by the infiltration of polycarbosilane or polymethylsilane solutions into various templates such as SiO_2 opals, mesoporous silica, and porous alumina membranes, followed by curing, pyrolysis and chemical etching steps, only a few studies of the preparation of SiC-related microparticles and their assemblies have been reported [10,16–19]. Tosheva et al. [20] prepared SiC particles by heat treating spherical ion-exchange resins impregnated with Si compounds. However, the particle size distribution was not uniform and it was impossible to fabricate a well-ordered SiC microparticles assembly. Kim et al. fabricated three-dimensional

* Corresponding author. Tel.: +81 92 682 1733; fax: +81 92 682 1733.
E-mail address: kusakabe@fwu.ac.jp (K. Kusakabe).

1385-8947/$ – see front matter © 2007 Elsevier B.V. All rights reserved.
doi:10.1016/j.cej.2007.04.028

ordered assemblies of SiC-based ceramic hollow spheres using carbon inverse opal structures as a template and polymethylsilane having a molecular weight of 580 as the SiC precursor [21]. The spheres partly expose the empty core through small holes on the shells, which is caused by the reduction in ceramic yield due to the low molecular weight of polymethylsilane [14].

Accordingly, a higher ceramic yield would be advantageous for fabricating denser ceramic products. In the present study, we chose polycarbosilane with a molecular weight as high as 1290 as precursor, which is generally synthesized from polymethylsilane and is frequently used as a SiC precursor [22]. Due to the higher molecular weight of this precursor, less weight loss and shrinkage would be expected and, as a result, the possible fabrication of microparticles and their assembly with good morphology. In the preparation process, a well-defined SiO_2 inverse opal was first prepared by the infiltration of a silica sol into the void of a PMMA opal structure. The polycarbosilane solution was infiltrated into SiO_2 inverse opal under reduced pressure. The influence of the viscosity of polycarbosilane solution on the morphologies of the final SiO_xC_y microparticles and their three-dimensional ordered assemblies was investigated.

2. Experimental

2.1. Fabrication of well-defined 3D SiO_2 inverse opal

Stable SiO_2 sol was prepared by the hydrolysis and condensation of tetraethylorthosilicate (TEOS). Chemical reagents, TEOS (96%, $Si(OC_2H_5)_4$; Tokyo Kasei Kogyo Co., LTD), absolute ethyl alcohol (EtOH; Wako), and hydrochloric acid (37% HCl; Wako) were used as received without further purification. TEOS was added dropwise to absolute EtOH, giving a clear solution. A small amount of dilute hydrochloric acid solution was added to the precursor solution followed by continuous stirring for the hydrolysis of TEOS. The molar composition of the sol was 1.0TEOS:20EtOH:0.02HCl:5H_2O. The sol was stable at room temperature for at least 5 months. However, its viscosity increased gradually with the hydrolysis time, and about 48 h later, the viscosity reached 2.0 mPa s, which is the optimum viscosity for fabricating a well-defined SiO_2 inverse opal.

A suspension of PMMA monodispersed particles was used for fabricating the opal structure. The particle size of PMMA was 260 nm. A small amount of PMMA suspension was dropped on the smooth bottom of a quartz plate. The gravitational sedimentation of PMMA monodisperse colloids and simultaneous drying resulted in a well-arranged artificial PMMA opal structure. The prepared opal was then treated at 90 °C for 24 h to permit the PMMA particles to come into contact with each. The infiltration of the prepared SiO_2 sol into the interstitial voids in the opal was then performed in a glove box filled with nitrogen. After a drying process for 24 h, the plate was heated to 550 °C at a rate of 1 °C/min and held for 10h in air. As a result of the burnout of the PMMA particles, a well-defined inverse SiO_2 opal was obtained.

2.2. Infiltration of polycarbosilane into SiO_2 inverse opal

Polycarbosilane (NIPUSI type-A, average molecular weight = 1290; Nihon Carbon Ltd.) as a precursor for preparing SiO_xC_y microparticles was dissolved in *p*-xylene (Aldrich). The concentration of the polycarbosilane solution was varied from 10 to 35 wt.% to control the viscosity of the infiltration solution. The viscosity was measured using a torsion-balanced, oscillation type viscometer (VM-1G, CBC Materials Co., Ltd., Japan). Tetrahydrofuran (THF, Aldrich) was also used as the solvent. The prepared SiO_2 inverse opal was then placed in a two-neck flask connected to a vacuum pump. After evacuation, the prescribed amount of polycarbosilane solution was injected into the inverse opal with a syringe through a rubber cap on the flask. The polycarbosilane that had infiltrated in the inverse opal was cured at 200 °C for 1 h in air. The cured sample was then heated to 1000 °C at a rate of 1 °C/min in dry N_2 and held for 1 h.

2.3. Silica dissolution in hydrofluoric acid and characterization

The obtained SiO_xC_y–SiO_2 composite was treated with an aqueous solution of HF for 24 h without stirring, followed by filtration and repeated washing with distilled water. The morphologies of the resulting SiO_xC_y microparticles and their assemblies were observed on a scanning electron micrograph (SEM, Hitachi, S-5200). Powder X-ray diffraction (XRD) patterns of the SiO_xC_y microparticles were recorded on a Rigaku RINT-2500 diffractometer using Cu Kα radiation. Diffraction patterns were referenced against the JCPDS database (card number 74-2307) for sample identification. IR spectra were measured using a Fourier transform infrared spectrometer (Perkin-Elmer, Spectrum One). The samples were first ground to a fine powder using a mortar and pestle, followed by mixing with KBr, and then pressed into pellets for the measurements. Nitrogen absorption–desorption measurements were done at 77 K on a Micrometritics ASAP 2010 gas sorptometer. Prior to the measurements, the samples were degassed at 140 °C for 12 h.

3. Results and discussion

Fig. 1 schematically illustrates the three-step approach for fabricating a SiO_xC_y microparticle assembly. As a first step, a well-ordered PMMA opal was formed through self-organization during natural evaporation after dropping the suspension of monodispersed PMMA microspheres on the substrate. In the second step, a SiO_2 inverse opal was prepared by infiltrating the silica sol into the void of the PMMA opal structure as a mold. PMMA particles were burned out during the calcination of the silica. In the final step, a solution of polycarbosilane in *p*-xylene was infiltrated into the SiO_2 inverse opal under reduced pressure. The polycarbosilane in the inverse opal was cured in air at 200 °C and pyrolyzed in deoxidized N_2 flow at 1000 °C. A SiO_xC_y microparticle assembly was finally fabricated by removing the SiO_2 framework from the composite materials of SiO_xC_y and SiO_2 in an HF solution.

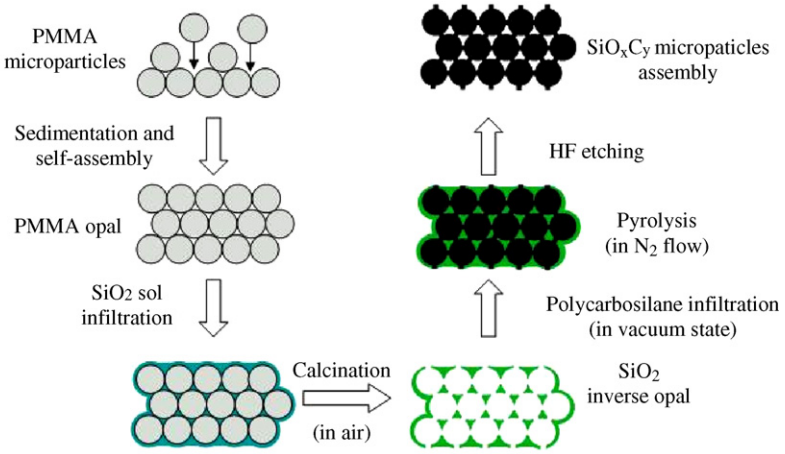

Fig. 1. Schematic illustration of the procedures for fabricating SiO_xC_y microparticles assembly.

A cross-section SEM image of the prepared PMMA opal is shown in Fig. 2(a). Monodispersed PMMA particles with a particle size of 260 nm were assembled into close-packed 3D colloidal crystals and extensively-piled up layer-by-layer on the smooth bottom of a small quartz vessel. It has been reported that monodispersed colloidal spheres sequently organize themselves into ordered 3D structures when they are subjected to physical confinement [23]. Herein, the quartz vessel served to physically confine the system, permitting colloidal spheres to be assembled into highly ordered structures in the confined vessel. During the preparation process, it was found that a slow evaporation is necessary to minimize the number of cracks that appear in the opal over a large area. Such cracks can form because the density of the particles in the resulting opal is greater than that in the original colloidal PMMA crystals. As shown in the inset of Fig. 2(a), the PMMA microspheres were hexagonally close-packed, and each particle was surrounded by six other particles. The interstices between the particles can be clearly observed and permit the SiO_2 sol to infiltrate into the opal in the later step.

Representative SEM images of the as-prepared well-defined SiO_2 inverse opal are depicted in Fig. 2(b). The inverse opal structure with highly ordered and interconnected honeycomb pores was obtained by replicating the three-dimensionally close-packed PMMA opal. The diameter of the spherical space in the inverse opal structure was about 230 nm as evaluated from the inset of Fig. 2(b), smaller than that of the 260 nm PMMA sacrificial sphere template, suggesting that about 11.5% shrinkage occurred during the calcination. Furthermore, the next lower layer inverse opal is visible in the inset SEM surface image. The small windows with a diameter of 60 nm formed inside the large spaces correspond to the contact points between the neighboring PMMA spheres. The connection of spaces through the

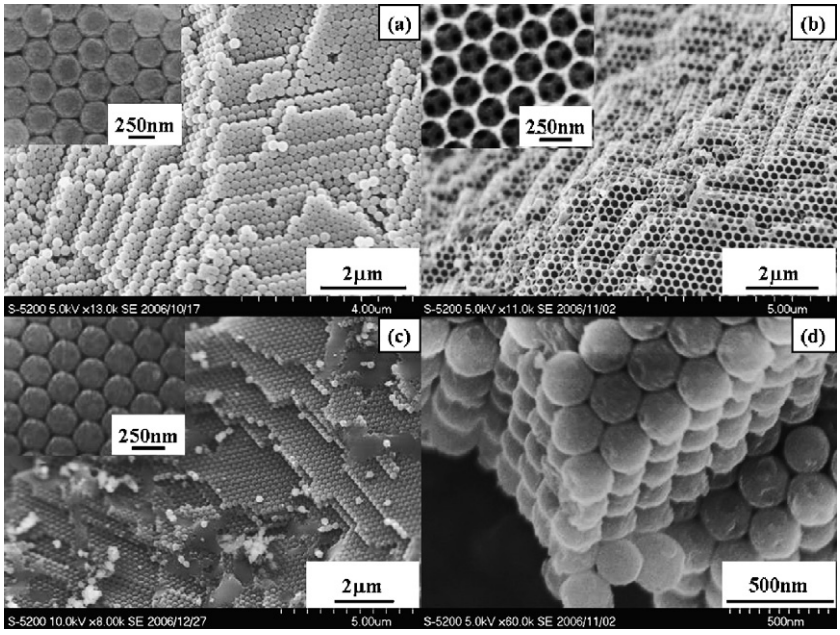

Fig. 2. Cross-sectional SEM images of (a) a prepared PMMA opal, (b) a SiO_2 inverse opal, (c) a replicated SiO_xC_y microparticle assembly and (d) its enlarged image. Insets show their enlarged SEM surface images.

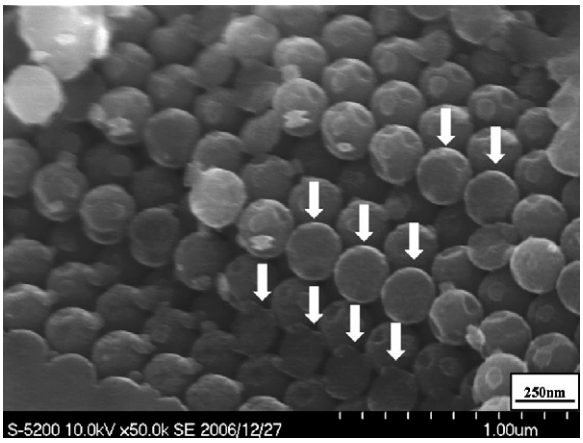

Fig. 3. Cross-sectional SEM images of a replicated SiO_xC_y microparticle assembly with some broken microparticles as shown by arrows.

windows is favorable for serving as templates for the subsequent replication process for preparing SiO_xC_y microparticles and their ordered assemblies. Thus the infiltration solution can easily reach the deeper layers. In addition, a one-step infiltration of the silica sol was found to be suitable for the formation of a continuous layer. When the viscosity of the silica sol was less than 2.0 mPa s, it was necessary to repeat the infiltration step. When the viscosity increased 2.5 mPa s, the sol was unable to infiltrate into the deep layer of the opal and a dense layer was usually formed on the surface after the calcination step. The silica sol with a viscosity of 2.0 mPa s filled the void very well using a one-step infiltration process.

Fig. 2(c and d) show cross-section images of a SiO_xC_y microparticle assembly formed using a 30 wt.% polycarbosilane solution with a corresponding viscosity of 2.03 mPa s. A well-ordered SiO_xC_y microparticle assembly was readily obtained and the shape of the particle assembly was almost a replica of the original close-packed PMMA microspheres. From the inset of Fig. 2(c), the SiO_xC_y microparticles are also hexagonally close-packed, and each particle is surrounded by six other particles. The interstices between the particles can be also clearly seen as those shown in the original PMMA opal. The particle size of SiO_xC_y was close to the diameter of the space of the SiO_2 inverse opal (230 nm), but smaller than that of a PMMA particle (260 nm), suggesting that the SiO_xC_y ceramic was substantially filled in the spherical space of the SiO_2 inverse opal after pyrolysis of the polycarbosilane. The arrows in Fig. 3 show some fractured sections of broken SiO_xC_y microparticles in the assembly after pressing, suggesting that the obtained microparticles are filled.

We used a linear polycarbosilane with a chemical composition of 50 wt.% Si, 40 wt.% C, 8.1 wt.% H, 0.5 wt.% O and 0.7 wt.% N. Its melting point was 232 °C in a N_2 atmosphere. To avoid melting, the polycarbosilane was cured in air at 200 °C for 1 h in order to produce cross-linked polymer networks composed of Si–O–Si bonds as shown in Scheme 1 [24–27]. The cured polycarbosilane becomes stable in air and are insoluble in solvents such as water and infusible for heating [27]. In the present study, the weight was increased by about 11% in this

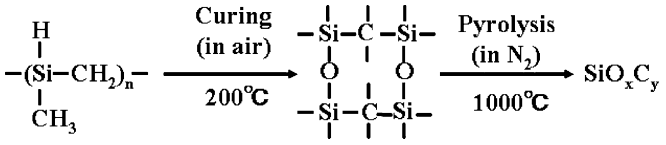

Scheme 1.

thermal oxidation step. Although the total weight loss of polycarbosilane after pyrolysis in a N_2 gas flow at 1000 °C for 1 h was about 15% due to the removal of organic groups, the particle size was not greatly reduced compared to the diameter of the space of the SiO_2 inverse opal as suggested above.

In order to investigate the chemical structure in detail, infrared spectra for as-received polycarbosilane, cured polycarbosilane, and the SiO_xC_y microparticle pyrolyzed at 1000 °C were collected. As illustrated in Fig. 4, the IR spectrum of the as-received polycarbosilane precursor shows typical absorption bands assigned to Si–H stretching (2100 cm^{-1}), Si–CH_3 deformation (1250 cm^{-1}), and Si–CH_2–Si (CH_2 wagging at 1020 cm^{-1} and 810 cm^{-1}). The IR spectrum of cured polycarbosilane shows significant reductions in absorption bands at 2100 and 1250 cm^{-1}, suggesting that a portion of the hydrogen and a certain amount of methyl groups were detached from the original polycarbosilane during the curing process. For the SiO_xC_y microparticle pyrolyzed at 1000 °C, the absorption bands corresponding to Si–H stretching and Si–CH_3 deformation completely disappeared, and the bands at 1020 and 810 cm^{-1} shifted to 1100 and 800 cm^{-1}, which can be attributed to the formation of Si–O bonds and Si–C bonds, respectively, suggesting that a silicon oxycarbide structure was created

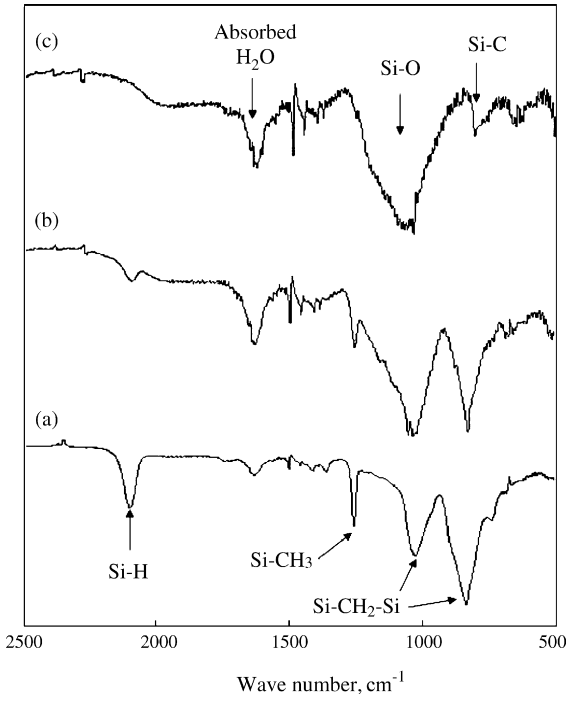

Fig. 4. IR spectra for (a) as-received polycarbosilane; (b) polycarbosilane cured at 200 °C in air for 1 h; (c) SiO_xC_y microparticle assembly pyrolyzed at 1000 °C in N_2 gas flow for 1 h.

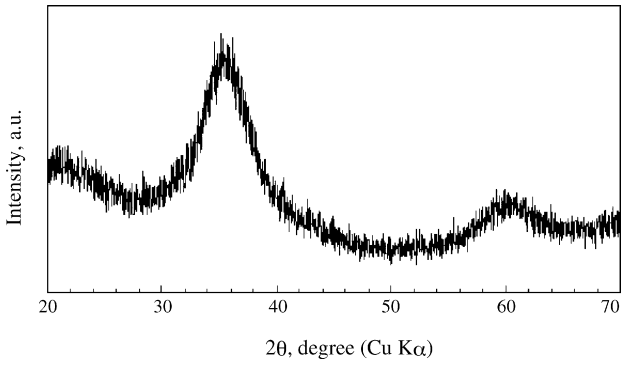

Fig. 5. X-ray diffraction pattern of as-prepared SiO_xC_y microparticle assembly pyrolyzed at 1000 °C in N_2 gas flow for 1 h.

[24–32]. The peak at 1610 cm^{-1} is due to adsorbed water because the measurement was performed in air [32].

The XRD pattern of the SiO_xC_y compound pyrolyzed at 1000 °C indicated broad peaks corresponding to β-SiC as shown in Fig. 5, suggesting that partial crystallization occurred even at this relatively low temperature in the present study. Using the Scherrer formula for the broad peak at 35.64°, the average grain size of SiC in the microparticles was estimated to be about 2 nm. Accordingly, nanocrystalline SiCs might be embedded in the amorphous SiO_xC_y matrix in the prepared microparticle assembly.

N_2 adsorption and desorption of the samples pyrolyzed at 1000 °C was performed, but no adsorption of N_2 was detectd, which is in agreement with the results reported in the literature [24,25]. This suggests that the surface of the obtained SiO_xC_y microparticles should have a dense structure.

SiO_xC_y microparticle assemblies were fabricated using a solution of polycarbosilane in *p*-xylene, at different concentrations. The viscosities of the solutions were 0.81, 0.97, 1.22, 1.59, 2.03 and 3.03 mPa s for 10, 15, 20, 25, 30 and 35 wt.% of polycarbosilane concentrations, respectively. The morphology of the as-fabricated SiO_xC_y microparticle assembly could be controlled by the viscosity of the polycarbosilane solution that was infiltrated. When the viscosity was less than 1.6 mPa s, the resulting SiO_xC_y microparticles were hollow particles. The broken structure of hollow SiO_xC_y microparticles is shown in Fig. 6(a). The particle size of the hollow microparticles was approximately 200 nm, much smaller than the diameter of the spherical space of a SiO_2 inverse opal, suggesting that the particle formed in the spherical space had shrunk due to the low concentration of solid components. Meanwhile, when the viscosity was above 3.0 mPa s, the solution infiltrated into spaces in the deeper layer of the SiO_2 inverse opal even at reduced pressure with great difficulty. As a result, a dense layer of SiO_xC_y consistently formed on the surface of the inverse opal as shown in Fig. 6(b). This image was also observed when a solution of polycarbosilane in tetrahydrofuran, with a lower boiling point (boiling point = 66 °C), was used. The rapid evaporation of THF during the infiltration process led to the formation of a polycarbosilane layer on the surface of SiO_2 before the infiltration.

SiO_xC_y microparticles were tightly connected to each other by SiO_xC_y bridges formed in the windows between the spherical spaces in the inverse opal. In order to observe the nanostructure of the SiO_xC_y microparticle assembly, the assembly was broken up by pressing. Some microspheres were released from the assembly as a microparticle as shown in Fig. 7(a). Fig. 7(b) shows the second layer of the SiO_xC_y microparticle assembly, and Fig. 7(c and d) shows the cross-section images inside the assembly observed from different observation angles. The SiO_xC_y bridges between the neighboring microparticles or traces of the removed bridges can be clearly seen on the remaining particles in the SiO_xC_y assembly, indicating by the numerals **1** and **2** in Fig. 7. In this assembly, twelve bridges are symmetrically formed on the surface of single microparticle inside the packed block. The diameter of the connecting bridges was about 60 nm and coincided with the connecting pore size in the SiO_2 inverse opal. These bridges significantly enhanced the mechanical strength of the fabricated SiO_xC_y microparticle assembly. Compared with the original PMMA opals, this assembly is disjointed with difficulty by sonication. Considering the voids formed in the 3-D well-ordered SiO_xC_y assembly, the diameter of the maximum circle formed at the intersections of three SiO_xC_y microparticles is 15.5% of the diameter of a microparticle and is calculated to be 35.6 nm in the present study, based on simple geometry. SiO_xC_y microparticle assemblies with interpores of different nanosizes could be also fabricated when the original PMMA microparticles with different sizes were used. This procedure offers a promising alternative to conventional nanofabrication for creating sieving structures for application to nanofluidic devices.

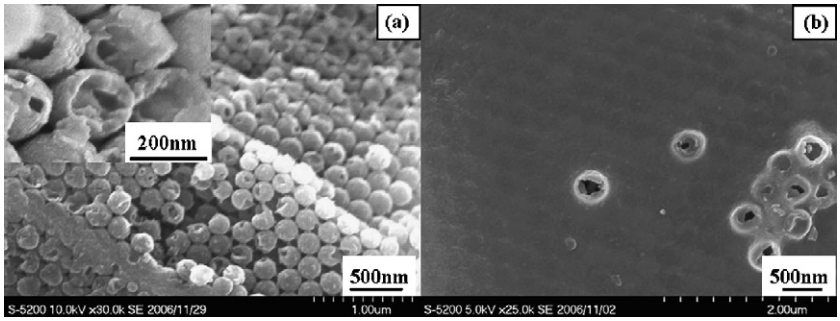

Fig. 6. SEM image of (a) the prepared SiO_xC_y microparticle assembly at a viscosity of 1.6 mPa s; (b) the surface state of polycarbosilane filled SiO_2 inverse opal pyrolyzed at 1000 °C for 1 h in a flow of N_2 gas at a viscosity of 3.03 mPa s.

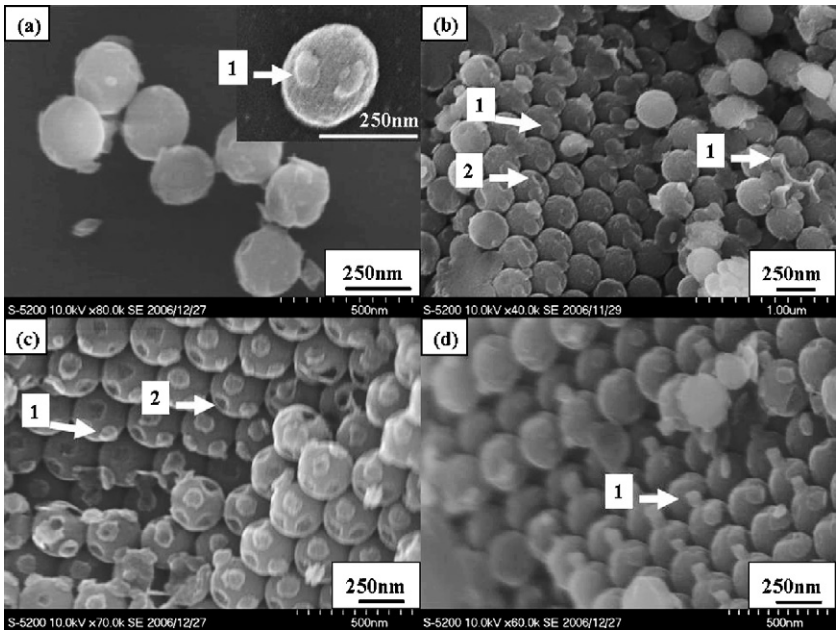

Fig. 7. SEM images of (a) discharged SiO_xC_y microparticles; (b) second layer of the SiO_xC_y microparticles assembly; (c and d) the cross-section images inside the assembly observed from different angles.

4. Conclusion

A simple process for fabricating robust, a high-quality 3D well-ordered SiO_xC_y microparticle assembly using home-made SiO_2 inverse opal as the mold and commercial polycarbosilane as the SiO_xC_y precursor is described. The obtained SiO_xC_y microparticle assembly has good morphology with a monodisperse particle size distribution and a controllable uniform pore size. To fabricate SiO_xC_y microparticles and their assemblies by one-step infiltration, the most suitable viscosity for the polycarbosilane solution was found to be approximately 2.0 mPa s for a one-step fabrication. The structure analysis showed that the obtained SiO_xC_y microparticles contained Si–O and Si–C bonds and SiC nanocrystals with a dense surface structure, and the mechanical strength of the SiO_xC_y microparticles assembly could be enhanced by bridge formation between the neighboring microparticles.

Acknowledgments

The authors would like to thank Prof. M. Kishida and Prof. S. Takenaka, Department of Chemical Engineering, Kyushu University for valuable discussions. This study was supported by Japan Society for the Promotion of Science (JSPS).

References

[1] P.V. Braun, S.A. Rinne, F. Garcia-Santamaria, Adv. Mater. 18 (2006) 2665.
[2] C. Lopez, Adv. Mater. 15 (2003) 1679.
[3] Y. Xia, B. Gates, Y. Yin, Y. Lu, Adv. Mater. 12 (2000) 693.
[4] F. Fleischhaker, A.C. Arsenault, V. Kitaev, F.C. Peiris, G. von Freymann, I. Manners, R. Zentel, G.A. Ozin, J. Am. Chem. Soc. 127 (2005) 9318.
[5] X. Xu, S.A. Asher, J. Am. Chem. Soc. 126 (2004) 7940.
[6] Z.T. Jiang, Y.M. Zuo, Anal. Chem. 73 (2001) 686.
[7] J. Feng, F. He, R. Zhuo, Macromolecules 35 (2002) 7175.
[8] H. Zhang, M.J. Wirth, Anal. Chem. 77 (2005) 1237.
[9] V.G. Pol, S.V. Pol, A. Gedanken, Chem. Mater. 17 (2005) 1797.
[10] T.H. Yoon, H.J. Lee, J. Yan, D.P. Kim, J. Ceram. Soc. Jpn. 114 (2006) 473.
[11] H. Zhang, C.G. Pantano, J. Am. Ceram. Soc. 73 (1990) 958.
[12] G.T. Burns, R.B. Taylor, Y. Xu, A. Zangvil, G.A. Zank, Chem. Mater. 4 (1992) 1313.
[13] F.I. Hurwitz, S.C. Farmer, F.M. Terepka, T.A. Leonhardt, J. Mater. Sci. 26 (1991) 1247.
[14] C.G. Pantano, A.K. Singh, H. Zhang, J. Sol-Gel Sci. Tech. 14 (1999) 7–25.
[15] A.K. Singh, C.G. Pantano, J. Am. Ceram. Soc. 79 (1996) 2696.
[16] S. Kwon, G. Son, J. Suh, K.T. Kim, J. Am. Ceram. Soc. 77 (1994) 3137.
[17] H. Wang, X.D. Li, J.S. Yu, D.P. Kim, J. Mater. Chem. 14 (2004) 1383.
[18] P. Krawiec, D. Geiger, S. Kaskel, Chem. Commun. (2006) 2469.
[19] K.H. Park, I.K. Sung, D.P. Kim, J. Mater. Chem. 14 (2004) 3436.
[20] L. Tosheva, J. Parmentier, S. Saadallah, C. Vix-Guterl, V. Valtchev, J. Patarin, J. Am. Chem. Soc. 126 (2004) 13624.
[21] H. Wang, J.S. Yu, X.D. Li, D.P. Kim, Chem. Commun. (2004) 2352.
[22] C.T. Nguyen, L.Y. Hong, D.P. Kim, J.Y. Lee, H.G. Woo, J. Ceram. Soc. Jpn. 114 (2006) 487.
[23] E. Kim, Y. Xia, G.M. Whitesides, J. Am. Chem. Soc. 118 (1996) 5722.
[24] Z. Li, K. Kusakabe, S. Morooka, J. Membr. Sci. 118 (1996) 159.
[25] L.L. Lee, D.S. Tsai, Ind. Eng. Chem. Res. 40 (2001) 612.
[26] K. Kaneko, K.I. Kakimoto, J. Non-Cryst. Solids 270 (2000) 181.
[27] K. Okamura, T. Shimoo, K. Suzuya, K. Suzuki, J. Ceram. Soc. Jpn. 114 (2006) 445–454.
[28] G.D. Soraru, F. Babonneau, J.D. Mackenzie, J. Mater. Sci. 25 (1990) 3886.
[29] E. Bouillon, F. Langlais, R. Pailler, R. Naslain, F. Cruege, P.V. Huong, J.C. Sarthou, A. Delpuech, C. Laffon, P. Lagarde, M. Monthioux, A. Oberlin, J. Mater. Sci. 26 (1991) 1333.
[30] E. Bouillon, D. Mocaer, J.F. Villeneuve, R. Pailler, R. Naslain, M. Monthioux, A. Oberlin, C. Guimon, G. Pfister, J. Mater. Sci. 26 (1991) 1517.
[31] Q. Liu, H.J. Wu, R. Lewis, G.E. Maciel, L.V. Interrante, Chem. Mater. 11 (1999) 2038.
[32] Q. Liu, W. Shi, F. Babonneau, L.V. Interrante, Chem. Mater. 9 (1997) 2434.